
SIG2TEXT, A VISION-LANGUAGE MODEL FOR NON-COOPERATIVE RADAR SIGNAL PARSING

Hancong Feng

School of Information and Communication Engineering
UEST of China
202211012303@std.uestc.edu.cn

KaiLi Jiang

School of Information and Communication Engineering
UEST of China
jiangkelly@foxmail.com

Bin tang

School of Information and Communication Engineering
UEST of China

April 17, 2025

ABSTRACT

Automatic non-cooperative analysis of intercepted radar signals is essential for intelligent equipment in both military and civilian domains. Accurate modulation identification and parameter estimation enable effective signal classification, threat assessment, and the development of countermeasures. In this paper, we propose a symbolic approach for radar signal recognition and parameter estimation based on a vision-language model that combines context-free grammar with time-frequency representation of radar waveforms. The proposed model, called Sig2text, leverages the power of vision transformers for time-frequency feature extraction and transformer-based decoders for symbolic parsing of radar waveforms. By treating radar signal recognition as a parsing problem, Sig2text can recognize the types and estimating the parameters of signals with arbitrarily complex modulations. We evaluate the performance of Sig2text on a synthetic radar signal dataset and demonstrate its effectiveness in various scenarios.

1 Introduction

Automatic non-cooperative analysis of intercepted radar signals plays a crucial role in intelligent systems for both military [38] and civilian applications [19, 2]. Accurate modulation identification and parameter estimation facilitate effective signal classification, threat assessment, and countermeasure development. However, the widespread adoption of software-defined radar systems [12, 4] has introduced new challenges. Modern radar systems employ advanced techniques such as low-power transmission, spread spectrum methods, frequency agility, and complex modulation schemes, significantly complicating signal analysis [21, 26].

Traditional approaches for radar signal intra-pulse modulation recognition and parameter estimation primarily rely on statistical signal processing techniques. Modulation recognition typically involves feature extraction followed by classification using statistical pattern recognition algorithms. For instance, [18] extracted features from Wigner and Choi-Williams time-frequency distributions and pruned redundant ones using an information-theoretic approach. Similarly, [36] decomposed signals into time-frequency atoms via a fast matching pursuit algorithm for robust emitter signature clustering. Decision-theoretic frameworks and statistical tests were introduced for intrapulse modulation recognition in [20, 31]. Parameter estimation methods have addressed challenges posed by low signal-to-noise ratios

and complex modern radar signals. [6] employed a cyclostationary approach to extract key modulation parameters of low probability of intercept (LPI) radar signals, achieving estimation errors below 6%. [3] reformulated chirp rate estimation as frequency estimation problems using multiple discrete polynomial phase transforms with optimal weighting. Additionally, [26] integrated time-frequency representations with visibility graph techniques for multicomponent LPI signal detection. Despite their effectiveness, these methods often depend on handcrafted features for specific signal types and struggle to adapt to emerging complex modulation schemes.

The rapid advancement of deep learning has led to numerous approaches, broadly categorized by their input: direct sampled sequences from analog-to-digital converters (ADCs) and time-frequency image representations. Sequence-based methods process sampled radar signals directly through neural networks for automatic feature extraction and modulation classification. Studies employing convolutional neural networks (CNNs) and long short-term memory (LSTM) networks have demonstrated promising results [16, 29, 25, 30]. Time-frequency image (TFI)-based approaches transform radar signals into time-frequency images before processing them with image-based neural networks. Specialized architectures [15, 23, 10, 11] have shown significant potential. For more complex scenarios involving overlapping signals or hybrid modulations, multi-label classification methods have been explored, including residual networks [13], multi-instance learning [22], feature pyramid networks with class activation mapping [24], and deep multi-label classifiers [34].

Existing methods primarily focus on intra-pulse modulation recognition without performing parameter estimation. To address this limitation, multi-task learning approaches have emerged. [1] proposed a multi-task learning technique using recurrent neural networks for joint SNR estimation, pulse detection, and modulation classification. [35] introduced JMRPE-Net, a deep multitask network for joint modulation recognition and parameter estimation of cognitive radar signals. For overlapped signals, [5] developed a joint semantic learning deep convolutional neural network that simultaneously performs feature restoration, modulation classification, and parameter regression. However, these models typically have fixed output heads, limiting their adaptability to signals with varying parameter counts and complex hybrid modulations.

This paper presents a symbolic approach for radar signal recognition and parameter estimation based on a vision-language model that combines context-free grammar (CFG) with time-frequency representations. Our proposed model, Sig2text, leverages vision transformers for time-frequency feature extraction and transformer-based decoders for symbolic waveform parsing. By framing radar signal recognition as a parsing problem, Sig2text effectively recognizes and parses waveforms with diverse modulation types and parameters. We evaluate Sig2text on a synthetic radar signal dataset, demonstrating its effectiveness in both recognition and parameter estimation.

The main contributions of this paper are:

- A symbolic radar signal representation method that compactly encodes arbitrary waveforms with varying parameters
- Sig2text, a novel architecture combining vision transformers for feature extraction with transformer-based decoders for symbolic parsing
- Comprehensive evaluation on synthetic radar signals, demonstrating effective type recognition and parameter estimation

2 Problem Formulation

2.1 Signal Model

For a non-cooperative radar signal receiver, the sampled signal $y(k)$ with additive white Gaussian noise (AWGN) can be modeled as:

$$y(k) = A \exp \left(j \cdot \left(\theta(k) + 2\pi \frac{f_c}{f_s} k \right) + \theta_p \right) + n(k) \quad (1)$$

where A denotes the constant signal amplitude within the pulse width, $\theta(k)$ represents the instantaneous phase, f_c is the carrier frequency, f_s is the sampling frequency, θ_p is the phase offset, and $n(k)$ is the AWGN component.

Based on the instantaneous phase $\theta(k)$, fundamental radar signals can be categorized into three primary types: frequency-modulated (FM), phase-coded (PC), and frequency-coded (FC) waveforms [4]. FM waveforms employ continuous phase modulation for pulse compression, with linear frequency modulation (LFM) being the most prevalent example. PC waveforms divide the pulse into constant-amplitude chips, each modulated by discrete phase values (either binary or polyphase). FC waveforms modulate their frequency according to predetermined stepped-frequency sequences, with Costas codes representing a common implementation. Table 1 summarizes these fundamental radar waveforms and their principal subclasses.

Table 1: Basic radar waveforms and their subclasses

Waveform Type	Subclasses
FM	LFM, Triangular Waveform (Tri)
PC	Barker, Polyphase, Frank, P1, P2, P3, P4
FC	Costas

Beyond these fundamental waveforms, practical radar systems often employ hybrid modulation schemes. For instance, combining FM and PC waveforms can produce signals like LFM/binary phase-shift keying (BPSK) to achieve low probability of interception. Similarly, integrating FC and PC waveforms enables effective jamming suppression [9]. Multiple LFM components with different slopes can also be combined to enhance velocity estimation in synthetic aperture radar (SAR) systems [33].

Given the exponential growth of possible signal combinations and their uncertain quantities, radar signal analysis cannot be adequately addressed as a simple classification or regression problem. We therefore formulate it as a parsing problem from the signal domain to the symbolic domain, as detailed in the following section.

2.2 The Task of Radar Signal Parsing

Similar to how humans use natural language with finite alphabets to describe image content, we can define a formal language to describe radar signals. Let Σ be a finite alphabet (a finite set of symbols), and let Σ^* denote the set of all finite strings over Σ :

$$\Sigma^* = \bigcup_{n=0}^{\infty} \Sigma^n,$$

where Σ^n represents all strings of length n (with $\Sigma^0 = \{\varepsilon\}$, where ε is the empty string). A *formal language* is any subset of Σ^* :

$$L \subseteq \Sigma^*.$$

Although the alphabet Σ is finite, Σ^* is infinite due to arbitrary symbol concatenation. This property provides formal languages with substantial expressive power, enabling the encoding of unlimited information. Furthermore, many formal languages employ grammars with recursive production rules, facilitating the construction of nested hierarchical structures necessary for representing complex syntactic patterns.

We formalize radar signal parsing as a mapping from continuous signals to discrete symbolic representations. Let a radar signal be represented by a vector

$$I \in \mathbb{R}^{N \times 1},$$

where N is the number of sample points. Given a finite alphabet Σ and the set of all finite strings Σ^* , the symbolic description of a radar signal is a sequence

$$T = (w_1, w_2, \dots, w_n) \in \Sigma^*,$$

where each $w_t \in \Sigma$. Our objective is to learn a mapping

$$f : \mathbb{R}^{N \times 1} \rightarrow \Sigma^*$$

by maximizing the conditional probability $P(T | I)$. Applying the chain rule yields the factorization:

$$P(T | I) = \prod_{t=1}^n P(w_t | I, w_1, \dots, w_{t-1}).$$

Thus, the parsing problem reduces to a conditional next-token prediction task, where learning f corresponds to estimating $P(w_t | I, w_1, \dots, w_{t-1})$ through neural network training.

The language design critically affects the clarity and conciseness of radar signal representation. In the following section, we present a specially designed language capable of representing arbitrary radar waveforms with varying parameters.

3 Method

This section first presents the symbolic representation of radar waveforms, then introduces the vision transformer architecture for time-frequency feature extraction and transformer-based decoders for symbolic parsing.

3.1 Symbolic Representation of Radar Waveforms

We describe an artificial language for representing arbitrary radar waveforms with varying parameters, enabling the formulation of radar signal recognition and parameter estimation as a language parsing problem.

The primary consideration is language type selection. While natural language descriptions are possible, they prove inefficient due to their extensive vocabularies (e.g., English or Chinese) and poor machine-parsability. Given the limited number of radar signal types and parameters, we employ a context-free grammar (CFG) for language design.

A CFG is a formal grammar where each production rule takes the form $A \rightarrow \alpha$, with A as a non-terminal symbol and α as a string of terminal and/or non-terminal symbols. The language generated by a CFG comprises all strings derivable from the start symbol through production rule applications. For instance, the CFG $G = (\{S\}, \{a, b\}, \{S \rightarrow aSb, S \rightarrow \epsilon\}, S)$ generates the language $\{a^n b^n | n \geq 0\}$. Despite their simple rules, CFGs can generate complex languages, as demonstrated in image processing [7] and multifunction radar modeling [28].

For basic waveforms (FM, phase-coded, and frequency-coded), our string representations follow the pattern: `<type> <sub> <parameter_list>`. The `type` field indicates the modulation category ('FM', 'PC', or 'FC'), while `sub_type` specifies the waveform variant (e.g., 'barker' under 'PC'). The `parameter_list` contains signal parameters like bandwidth, carrier frequency, and code sequences. Table 2 presents the grammar rules. For example:

- FM LFM cf 100.0 B 10.0 denotes a linear FM waveform with 100.0 MHz center frequency and 10.0 MHz bandwidth
- FC Costas cf 100.0 FH 1.0 Code 7 6 2 10 1 4 8 9 11 5 3 represents a Costas-coded waveform with 100.0 MHz center frequency, 1.0 MHz frequency hop, and specified code sequence

Table 2: Grammar rules for five basic radar waveforms (LFM, P1, P2, P4, CostasFM). Terminal symbols: `< FM >`, `< PM >`, `< FC >`, `< P1 >`, `< P2 >`, `< P4 >`, `< Costas >`, `< LFM >` (waveform types); `< cf >`, `< B >`, `< FH >`, `< Code >` (estimated parameters); `< FLOAT >`, `< INT >` (parameter values).

Non-terminal	Productions
<code>< ENTRY ></code>	<code>< FM_ENTRY > < PM_ENTRY > < FC_ENTRY ></code>
<code>< FM_ENTRY ></code>	<code>< FM > < LFM > < cf > < FLOAT > < B > < FLOAT ></code>
<code>< PM_ENTRY ></code>	<code>< PM > < P_TYPE > < cf > < FLOAT > < code_length > < INT ></code>
<code>< FC_ENTRY ></code>	<code>< FC > < Costas > < cf > < FLOAT > < FH > < FLOAT > < Code > < INT_LIST ></code>
<code>< P_TYPE ></code>	<code>< P1 > < P2 > < P4 ></code>
<code>< INT_LIST ></code>	<code>< INT > < INT_LIST > < INT ></code>

Composite waveforms are handled through recursive grammar rules by adding `< S > → < ENTRY > < S > | < ENTRY >`. For example, FM LFM cf 100.0 B 10.0 PM P1 cf 100.0 code_length 10 combines LFM and P1 waveforms with repeated carrier frequency (only the first occurrence is retained during parsing).

Continuous parameter values (e.g., `< FLOAT >`) require quantization into discrete tokens for decoder compatibility. The quantization process involves dividing by an appropriate unit and rounding to the nearest integer. For instance, with a 0.1 MHz quantization unit, a 23.43 MHz bandwidth becomes token 234.

3.2 Architecture of Sig2text

To enhance feature interpretability and noise robustness, we first apply time-frequency transformation to radar waveforms before encoder processing. For computational efficiency, we employ the Short-Time Fourier Transform (STFT), retaining only the magnitude component which contains the most salient information, resulting in single-channel time-frequency representations.

While convolutional neural networks (CNNs) have traditionally dominated time-frequency image processing, their limited receptive fields constrain their ability to capture long-range dependencies. To overcome this limitation, we adopt the Vision Transformer (ViT) [8], which processes images as sequences of patches through transformer encoders. This architecture enables global receptive fields through self-attention mechanisms, demonstrating superior performance in various vision tasks including recognition and segmentation [32].

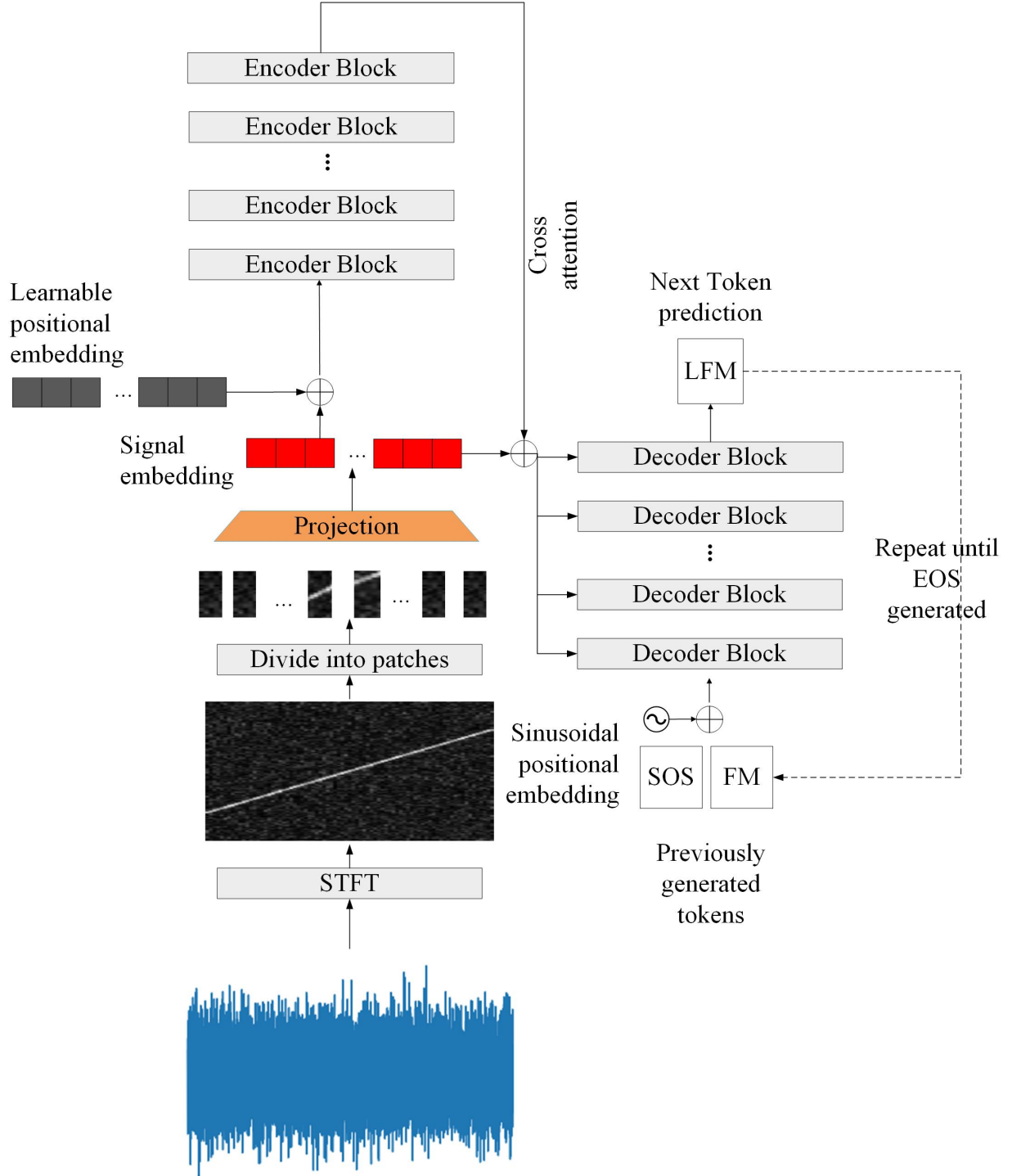


Figure 1: Architecture overview of Sig2text, demonstrating the complete processing pipeline from raw signal input to symbolic output.

3.3 Training and Inference

Given a dataset of radar signals $\{x^{(i)}\}_{i=1}^N$ with corresponding symbolic representations $\{s^{(i)}\}_{i=1}^N$, our objective is to learn model parameters θ that maximize the conditional likelihood:

$$\mathcal{L}(\theta) = \frac{1}{N} \sum_{i=1}^N \log p_{\theta}(s^{(i)} | x^{(i)}) \quad (2)$$

Direct likelihood maximization through autoregressive prediction can be computationally inefficient. We therefore employ teacher forcing during training, using ground truth tokens as decoder inputs rather than model predictions. This yields the training objective:

$$\mathcal{L}_{\text{TF}}(\theta) = -\frac{1}{N} \sum_{i=1}^N \sum_{t=1}^{T_i} \log p_{\theta}(s_t^{(i)} | s_{<t}^{(i)}, x^{(i)}) \quad (3)$$

where T_i denotes the length of $s^{(i)}$, and $p_{\theta}(s_t^{(i)} | s_{<t}^{(i)}, x^{(i)})$ represents the conditional probability of token $s_t^{(i)}$ given previous tokens $s_{<t}^{(i)} = (s_1^{(i)}, \dots, s_{t-1}^{(i)})$ and input $x^{(i)}$. We optimize this objective via gradient descent, with the complete training procedure outlined in Algorithm 1. Special tokens $\langle \text{sos} \rangle$ and $\langle \text{eos} \rangle$ mark the start and end of each string respectively.

Algorithm 1 Model Training Procedure

Require: Training set $\mathcal{D} = \{(x^{(i)}, s^{(i)})\}_{i=1}^N$, learning rate η , epochs E , batch size B

- 1: Quantize continuous parameters in $s^{(i)}$ to discrete tokens
 - 2: Augment strings with $\langle \text{sos} \rangle$ and $\langle \text{eos} \rangle$ tokens; construct vocabulary
 - 3: **for** $epoch = 1$ **to** E **do**
 - 4: **for** each mini-batch $\mathcal{B} \subset \mathcal{D}$ **do**
 - 5: Compute STFT magnitude spectra for signals x
 - 6: Partition time-frequency images into patches; project to D -dim embeddings
 - 7: Incorporate learnable positional encodings
 - 8: Encode patches via Transformer encoder
 - 9: Predict next-token distributions using Transformer decoder
 - 10: Compute negative log-likelihood loss (equivalent to cross-entropy)
 - 11: Update parameters via gradient descent with learning rate η
 - 12: **end for**
 - 13: **Optional:** Evaluate on validation set
 - 14: **end for**
-

During inference, we employ beam search decoding with width K to generate predictions. The algorithm maintains K most probable partial sequences at each step, expanding and pruning candidates until termination conditions are met. The complete inference process is detailed in Algorithm 2.

Algorithm 2 Beam Search Inference

Require: Input signal x , beam width K , maximum length T_{\max}

- 1: Compute STFT magnitude spectrum of x
- 2: Process time-frequency image through patch embedding layer
- 3: Add positional encodings
- 4: Generate latent representation via Transformer encoder
- 5: Initialize beam with $\langle \text{sos} \rangle$ token
- 6: **for** $t = 1$ **to** T_{\max} **do**
- 7: **for** each partial sequence in beam **do**
- 8: Predict next-token distribution using decoder
- 9: Compute sequence log-likelihoods
- 10: Expand partial sequences with candidate tokens
- 11: **end for**
- 12: Retain top- K sequences by likelihood
- 13: **if** any sequence terminates with $\langle \text{eos} \rangle$ **then**
- 14: Break
- 15: **end if**
- 16: **end for**
- 17: Return highest-likelihood sequence, converting tokens to waveform parameters

4 Simulations

This section evaluates the performance of our proposed Sig2text model on synthetic radar signal datasets. We assess the model’s capabilities in both type recognition and parameter estimation, while also examining its robustness and transfer learning potential for real-world applications. The PyTorch implementation is publicly available¹.

4.1 Dataset Description

We evaluate our model using synthetic datasets generated by a CUDA-based radar simulator that models the complete transmission and reception chain. The ADC receiver is 100 MHz with 8-bits effective precision. The pulse widths of the emitter ranging from 50 μs to 100 μs . Due to different Effective Radiated Power(ERP) and distance from the emitter to the receiver, the signal-to-noise ratio (SNR) of the signals varies from -10dB to 10dB.

Our first dataset contains 500,000 samples uniformly distributed across 13 classes:

- Frequency modulation: LFM, sinusoidal (Sin), triangular (Tri)
- Phase coding: Frank, P1-P4, T1-T4
- Frequency coding: Costas

Table 3 details the parameter ranges for each modulation type. All parameters were randomly generated within these specified bounds.

Table 3: Parameter Ranges for LPI Radar Signals

Parameter	Range	Applicable Signals	Description
cf	10–40 MHz	All	Center frequency
B	2–20 MHz	LFM: 2–10; Sin/Tri: 10–20	Bandwidth
T	5–20 μs	Sin/Tri	Modulation period
FH	≥ 0.5 MHz	Costas	Frequency hop step
segment_num	1–4	T1-T4	Segment count
phasetate_num	2–4	T1-T4	Phase states
ΔF	1–10 MHz	T3/T4	Modulation bandwidth
code_length	3–10	P1-P4	Code length
Code	-	Costas	Costas sequences

The second dataset extends the first by adding 500,000 hybrid modulation samples. These combine fundamental waveforms through various composition methods, as detailed in Table 4.

Table 4: Hybrid Modulation Combinations

Hybrid Type	Components	Combination Method
FM+FM	Multiple LFM	Sequential
FM+PM	LFM + Polyphase (P1-4, T1-4, Frank)	Multiplicative
FM+FC	LFM + Costas	Multiplicative
PM+FC	Polyphase + Costas	Multiplicative
PM+PM	Two Polyphase (P1-4, Frank)	Sequential

4.2 Hyperparameters and Baseline Methods

This section details the experimental hyperparameters and baseline methods used for comparative evaluation.

Since existing baselines cannot perform complete signal recognition and parameter estimation for hybrid modulations, we compare full functionality only for basic modulations. For hybrid modulations, we evaluate only recognition performance. The baseline methods include:

- **JMRPE-Net [35]**: A multi-task network combining CNN, LSTM, and self-attention modules for joint modulation recognition and parameter estimation.
- **MTViT**: A vision transformer encoder with fixed output heads, used to validate the feature extraction capability of our encoder architecture.
- **ResNet-based Multi-Label Classifier [13]**: A CNN model employing residual blocks for time-frequency feature extraction, trained with multi-label classification loss.

Table 5 summarizes the key hyperparameters for all models. We employ smaller Sig2text variants for single modulations and larger ones for hybrid modulations.

Table 5: Model Architecture Hyperparameters

Component	JMRPE-Net	MTViT	Sig2text-S	Sig2text-L
CNN Layers	3 layers (1,64,7) → (64,128,5) → (128,256,3)	-	-	-
LSTM	Bidirectional Input: 256 Hidden: 128	-	-	-
Attention	8-head Hidden: 256	8-head Hidden: 128	8-head Hidden: 128	8-head Hidden: 512
Transformer Encoder	-	3 layers Hidden: 128 FF: 512	3 layers Hidden: 128 FF: 512	6 layers Hidden: 512 FF: 1024
Transformer Decoder	-	-	3 layers Hidden: 128 FF: 512	6 layers Hidden: 512 FF: 1024

For Sig2text, we implement the CFG rules shown in Table 6 to generate symbolic signal descriptions. Continuous values are quantized with 0.01 resolution. During inference, we use beam search with size 1 and maximum output length 50. To convert the produced string into types and parameters, the bottom-up parsing [14] algorithm is employed.

All models were trained using AdamW optimizer [17] with batch size 128 and initial learning rate 0.001, reduced by 0.5 every 20 epochs. We reserved 3,000 samples for validation, stopping training when validation loss plateaued for 10 epochs. The hardware used for training included a single NVIDIA A100 GPU with 40GB memory.

4.3 Results and Discussion

The models are evaluated on the test set using two key metrics: (1) the accuracy of type/code recognition and (2) the mean square error (MSE) of parameter estimation. These metrics are defined as follows:

$$\text{Accuracy} = \frac{\text{Number of correct predictions}}{\text{Total number of predictions}} \quad (4)$$

Table 6: CFG Rules for Radar Signal Description

Non-Terminal	Production Rule
S	$SimpleString \mid S \ SimpleString$
$SimpleString$	$TypeChoice \ SubTypeChoice \ para$
$TypeChoice$	"FM" "PM" "FC"
$SubTypeChoice$	"LFM" "Sin" "Tri" "Costas" "T1-T4" "P1-P4"
$para$	$LFMpara \mid SinTripara \mid Costaspara \mid T12para \mid T34para \mid Ppara$
$LFMpara$	"cf" Cf "B" Bv
$SinTripara$	"cf" Cf "B" Bv "T" Tv
$Costaspara$	"cf" Cf "FH" FHv "Code" CS
$T12para$	"cf" Cf "seg_num" SN "phasestate_num" PSN
$T34para$	"cf" Cf "seg_num" SN "phasestate_num" PSN "deltaF" DF
$Ppara$	"cf" Cf "code_length" CL
Cf	$Number$
Bv	$Number$
Tv	$Number$
FHv	$Number$
CS	$Number \mid Number \ " \ " \ CS$
SN	$Number$
PSN	$Number$
DF	$Number$
CL	$Number$
SCL	$Number$

$$MSE = \frac{1}{N} \sum_{i=1}^N (\hat{para}_i - para_i)^2 \quad (5)$$

where \hat{para}_i denotes the predicted parameter value and $para_i$ represents the ground truth. A prediction is considered correct only if all possible types/codes in a signal are accurately identified. Incorrect predictions are excluded from MSE calculations.

We first evaluate the models using the radar simulator, generating 1000 samples of 13 basic radar waveforms with uniform distribution at 0 dB SNR. The results, presented in Table 7, demonstrate that Sig2text consistently outperforms both JMRPENet and MTvit across most parameters, achieving significantly lower MSE values—particularly for frequency-domain parameters (cf and B). However, MTvit exhibits superior performance in estimating the number of segments in T codes, where both Sig2text and JMRPENet show limitations. This performance discrepancy may arise from two key factors: (1) the difference in loss functions (Sig2text employs token-prediction-based cross-entropy loss, while MTvit uses regression loss) and (2) the distinct input features, with MTvit leveraging STFT results that demonstrate stronger noise robustness compared to JMRPENet.

For type recognition accuracy, the STFT-based approach achieves near-perfect classification performance (0.999), whereas JMRPENet trails with 0.944 accuracy. This result confirms that time-frequency image (TFI) processing maintains an advantage over raw sequence processing for modulation classification tasks.

Table 7: Performance comparison of different methods at SNR = 0 dB

Metric	Sig2text	JMRPENet	MTvit
cf	0.0003	0.0203	0.6852
B	0.0053	0.0222	0.1441
T	0.0034	0.0031	0.0980
segment_num	1.4759	1.7730	0.1683
phasestate_num	0.0214	0.1639	0.1239
FH	0.0001	0.0093	0.0217
code_length	0.0000	0.0358	0.0250
deltaF	0.0098	0.0010	0.0024
Type Accuracy	0.999	0.944	0.996

To further assess performance across varying noise conditions, we test the models at SNR levels ranging from -10 dB to 10 dB. Figures 2 and 3 present the results for type recognition accuracy and the MSE of key parameters (*cf*, *B*, *T*, and *segment_num*). Sig2text maintains superior parameter estimation performance for most metrics, though it struggles with segment number estimation. Notably, JMRPENet’s performance improves with increasing SNR, supporting our initial hypothesis.

Figure 3a reveals that Sig2text achieves consistently higher type recognition accuracy across all SNR levels, maintaining over 94% accuracy even at -10 dB. In contrast, JMRPENet shows strong SNR dependence, with accuracy dropping to 66% at -10 dB but matching other models at 5 dB and above. This further validates the robustness of TFI-based features in noisy environments. Additionally, Sig2text demonstrates exceptional performance for Costas code sequences, achieving perfect estimation above -2.5 dB and maintaining reasonable robustness at lower SNR levels.

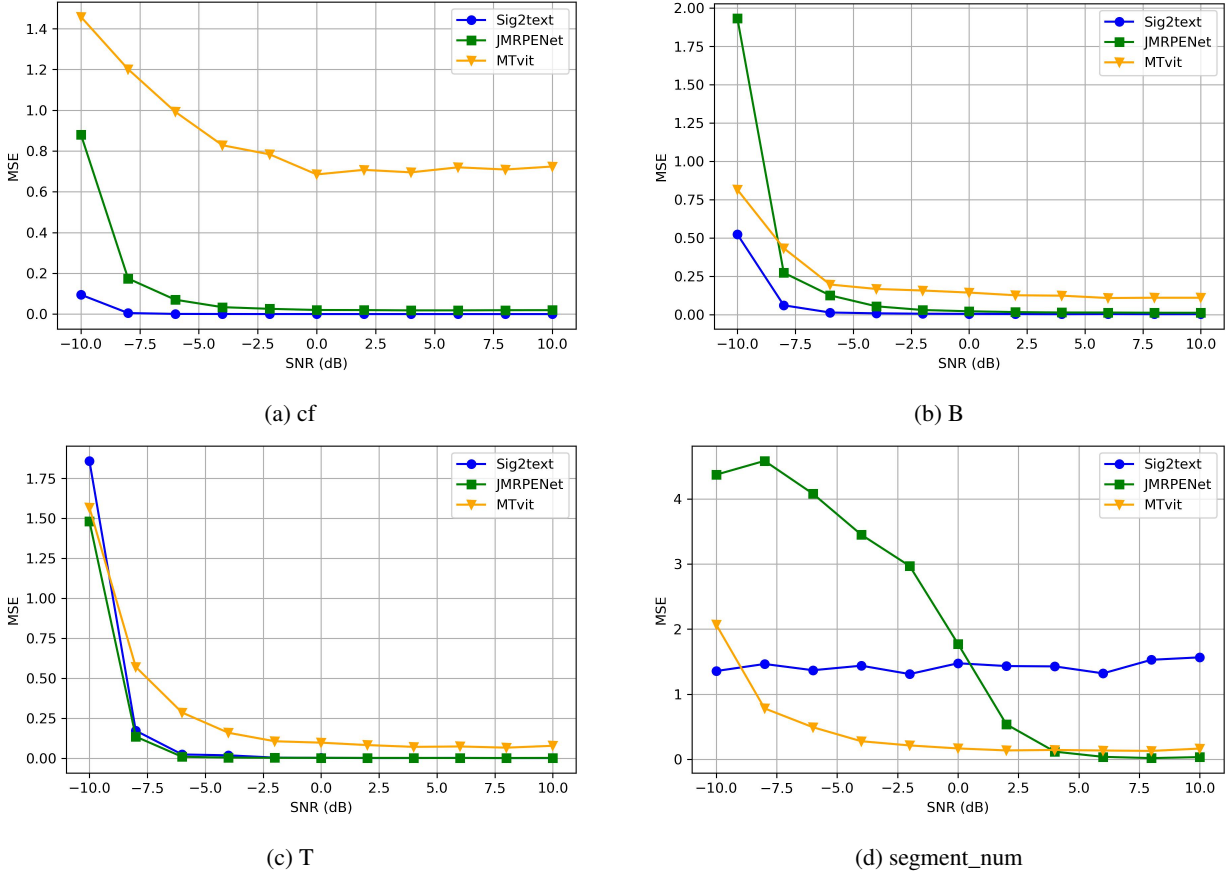
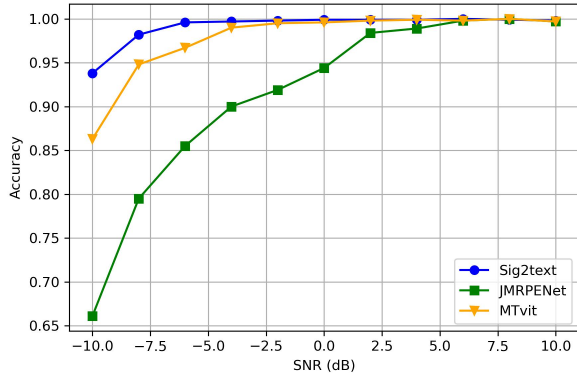


Figure 2: Parameter estimation performance across different SNR levels.

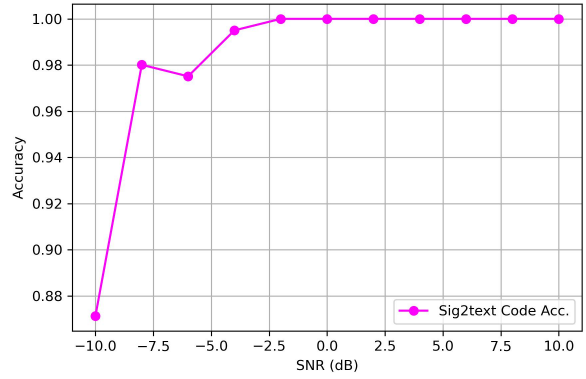
Next, we evaluate the models on hybrid modulation signals. Using the same evaluation protocol, we report type recognition accuracy and parameter estimation MSE for different signal combinations (Fig. 4). Sig2text-Large outperforms ResNet-Multi-Label across all combinations. Furthermore, it successfully processes same-type combinations while maintaining accurate parameter estimation.

Finally, we examine the models’ transfer learning capability by replacing linear frequency modulation (LFM) with sinusoidal modulation in Table 3 and fine-tuning with varying amounts of training data (Fig. 5). Sig2text significantly outperforms multi-label ResNet, particularly with limited training samples, suggesting that its vision-language learning paradigm extracts more generalizable features.

We also measure inference speed by processing one sample of length 0.1ms on an NVIDIA A100 GPU with a batch size of 128 (Table 8). Non-autoregressive models (Mvit, ResNet-Multi-Label, JMRPE-Net) achieve real-time processing, while Sig2text is slower due to its larger size and autoregressive decoding. However, model compression techniques [37] (e.g., quantization and pruning) could enable real-time operation.

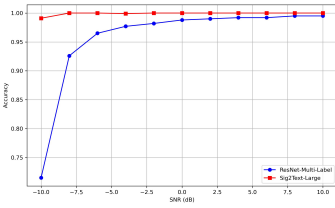


(a) Type Recognition Accuracy

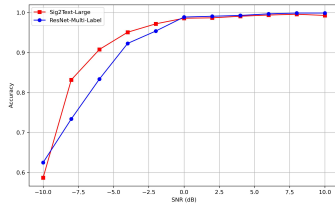


(b) Code Estimation Accuracy

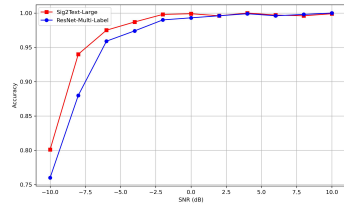
Figure 3: Accuracy comparison and Sig2text code estimation performance.



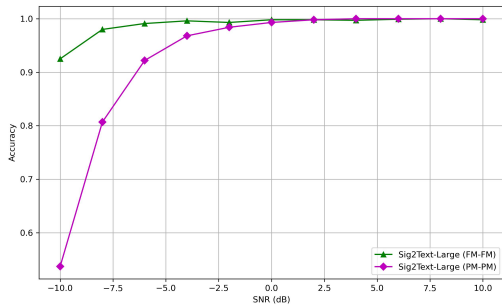
(a) FM-FC Accuracy



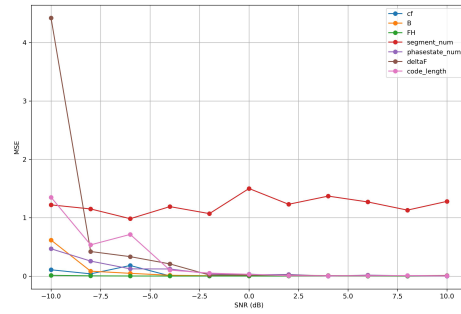
(b) FM-PC Accuracy



(c) PC-FC Accuracy



(d) FM-FM and PM-PM Accuracy



(e) All Combinations - Parameters MSE

Figure 4: Performance comparison between ResNet-Multi-Label and Sig2Text-Large. (a-c) Recognition accuracy for different signal combinations. (d) Accuracy of Sig2Text-Large for FM-FM and PM-PM combinations. (e) Parameter estimation MSE across all combinations.

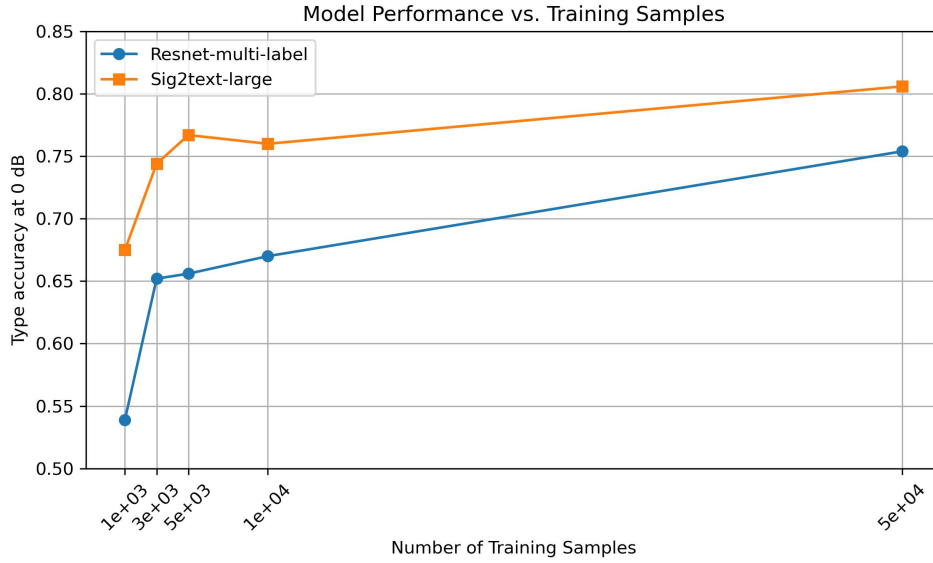


Figure 5: Type recognition accuracy after fine-tuning with different training sample sizes.

Table 8: Inference speed (including STFT computation) of different models

Model	Inference Speed	Model Inputs
Sig2text	0.8 ms	STFT magnitude patches
Sig2text-Large	4 ms	STFT magnitude patches
MViT	0.020 ms	STFT magnitude patches
ResNet-Multi-Label	0.045 ms	STFT magnitude
JMRPE-Net	0.015 ms	Raw waveform

5 Conclusion

In this paper, we propose Sig2text, a unified approach for radar signal recognition and parameter estimation. The method employs a Vision Transformer architecture to extract time-frequency features from radar signals, coupled with a transformer-based decoder that parses symbolic representations defined by a CFG. We evaluate the proposed method on a synthetic radar signal dataset and compare its performance against baseline approaches. Experimental results demonstrate that Sig2text achieves superior performance in both signal type recognition and parameter estimation tasks. Furthermore, the model exhibits strong transfer learning capabilities, suggesting its ability to learn generalizable feature representations.

Several promising directions exist for future research. First, the method could be extended to perform signal detection tasks by augmenting the CFG productions with additional tokens representing pulse boundaries (e.g., $\langle \text{toa} \rangle$ and $\langle \text{toe} \rangle$). Second, similar to the representation of hybrid modulations, the CFG could be further expanded to accommodate overlapping signals, thereby enabling the model to handle more complex real-world scenarios.

References

- [1] Fatih Çağatay Akyön, Mustafa Atahan Nuhoglu, Yaşar Kemal Alp, and Orhan Arıkan. Multi-Task Learning Based Joint Pulse Detection and Modulation Classification. In *2019 27th Signal Processing and Communications Applications Conference (SIU)*, pages 1–4, April 2019.
- [2] Canan Aydogdu, Musa Furkan Keskin, Gisela K Carvajal, Olof Eriksson, Hans Hellsten, Hans Herbertsson, Emil Nilsson, Mats Rydstrom, Karl Vanas, and Henk Wymeersch. Radar interference mitigation for automated driving: Exploring proactive strategies. *IEEE Signal Processing Magazine*, 37(4):72–84, 2020.

- [3] Guo Bai, Yufan Cheng, Wanbin Tang, and Shaoqian Li. Chirp Rate Estimation for LFM Signal by Multiple DPT and Weighted Combination. *IEEE Signal Processing Letters*, 26(1):149–153, January 2019.
- [4] Shannon D. Blunt and Eric L. Mokole. Overview of radar waveform diversity. *IEEE Aerospace and Electronic Systems Magazine*, 31(11):2–42, November 2016.
- [5] Kuiyu Chen, Lipo Wang, Jingyi Zhang, Si Chen, and Shuning Zhang. Semantic Learning for Analysis of Overlapping LPI Radar Signals. *IEEE Transactions on Instrumentation and Measurement*, 72:1–15, 2023.
- [6] Raja Kumari Chilukuri, Hari Kishore Kakarla, and K. Subbarao. Estimation of Modulation Parameters of LPI Radar Using Cyclostationary Method. *Sensing and Imaging*, 21(1):51, October 2020.
- [7] Freddy C Chua and Nigel P Duffy. DeepCPCFG: Deep learning and context free grammars for end-to-end information extraction. In *International Conference on Document Analysis and Recognition*, pages 838–853. Springer, 2021.
- [8] Alexey Dosovitskiy, Lucas Beyer, Alexander Kolesnikov, Dirk Weissenborn, Xiaohua Zhai, Thomas Unterthiner, Mostafa Dehghani, Matthias Minderer, Georg Heigold, Sylvain Gelly, et al. An image is worth 16x16 words: Transformers for image recognition at scale. *arXiv preprint arXiv:2010.11929*, 2020.
- [9] Zhiting Fei, Jiachen Zhao, Zhe Geng, Xiaohua Zhu, and Jindong Zhang. Hybrid FSK-PSK Waveform Optimization for Radar Based on Alternating Direction Method of Multiplier (ADMM). *Sensors*, 21(23):7915, January 2021.
- [10] Qiang Guo, Xin Yu, and Guoqing Ruan. LPI Radar Waveform Recognition Based on Deep Convolutional Neural Network Transfer Learning. *Symmetry*, 11(4):540, April 2019.
- [11] Yuanpu Guo, Haixin Sun, Hui Liu, and Zhenmiao Deng. Radar Signal Recognition Based on CNN With a Hybrid Attention Mechanism and Skip Feature Aggregation. *IEEE Transactions on Instrumentation and Measurement*, 73:1–13, 2024.
- [12] Sevgi Zubeyde Gurbuz, Hugh D. Griffiths, Alexander Charlish, Muralidhar Rangaswamy, Maria Sabrina Greco, and Kristine Bell. An Overview of Cognitive Radar: Past, Present, and Future. *IEEE Aerospace and Electronic Systems Magazine*, 34(12):6–18, December 2019.
- [13] Yu Hong-hai, Yan Xiao-peng, Liu Shao-kun, Li Ping, and Hao Xin-hong. Radar emitter multi-label recognition based on residual network. *Defence Technology*, 18(3):410–417, March 2022.
- [14] John E Hopcroft, Rajeev Motwani, and Jeffrey D Ullman. Introduction to automata theory, languages, and computation. *Acm Sigact News*, 32(1):60–65, 2001.
- [15] Thien Huynh-The, Van-Sang Doan, Cam-Hao Hua, Quoc-Viet Pham, Toan-Van Nguyen, and Dong-Seong Kim. Accurate LPI Radar Waveform Recognition With CWD-TFA for Deep Convolutional Network. *IEEE Wireless Communications Letters*, 10(8):1638–1642, August 2021.
- [16] Zehuan Jing, Peng Li, Bin Wu, Shibo Yuan, and Yingchao Chen. An Adaptive Focal Loss Function Based on Transfer Learning for Few-Shot Radar Signal Intra-Pulse Modulation Classification. *Remote Sensing*, 14(8):1950, January 2022.
- [17] Ilya Loshchilov and Frank Hutter. Decoupled weight decay regularization. In *International Conference on Learning Representations*.
- [18] Jarmo Lunden and Visa Koivunen. Automatic Radar Waveform Recognition. *IEEE Journal of Selected Topics in Signal Processing*, 1(1):124–136, June 2007.
- [19] Dingyou Ma, Nir Shlezinger, Tianyao Huang, Yimin Liu, and Yonina C Eldar. Joint radar-communication strategies for autonomous vehicles: Combining two key automotive technologies. *IEEE signal processing magazine*, 37(4):85–97, 2020.
- [20] Jin Ming, Sheng xulong, and Hu Guobing. Intrapulse modulation recognition of radar signals based on statistical tests of the time-frequency curve. In *Proceedings of 2011 International Conference on Electronics and Optoelectronics*, volume 1, pages V1–300–V1–304, July 2011.
- [21] Phillip E. Pace. *Detecting and Classifying Low Probability of Intercept Radar*. Artech House Radar Library. Artech House, Boston, 2nd ed edition, 2009.
- [22] Zesi Pan, Shafei Wang, Mengtao Zhu, and Yunjie Li. Automatic waveform recognition of overlapping LPI radar signals based on multi-instance multi-label learning. *IEEE Signal Processing Letters*, 27:1275–1279, 2020.
- [23] Zhiyu Qu, Wenyang Wang, Changbo Hou, and Chenfan Hou. Radar signal intra-pulse modulation recognition based on convolutional denoising autoencoder and deep convolutional neural network. *IEEE Access*, 7:112339–112347, 2019.

- [24] Weijian Si, Jiayi Luo, and Zhian Deng. Multi-label hybrid radar signal recognition based on a feature pyramid network and class activation mapping. *IET Radar, Sonar & Navigation*, 16(5):786–798, 2022.
- [25] Jun Sun, Guangluan Xu, Wenjuan Ren, and Zhiyuan Yan. Radar emitter classification based on unidimensional convolutional neural network. *IET Radar, Sonar & Navigation*, 12(8):862–867, August 2018.
- [26] Wan Tao, Jiang Kaili, Liao Jingyi, Jia Tingting, and Tang Bin. Research on LPI radar signal detection and parameter estimation technology. *Journal of Systems Engineering and Electronics*, 32(3):566–572, June 2021.
- [27] Ashish Vaswani, Noam Shazeer, Niki Parmar, Jakob Uszkoreit, Llion Jones, Aidan N Gomez, Łukasz Kaiser, and Illia Polosukhin. Attention is All you Need. In *Advances in Neural Information Processing Systems*, volume 30. Curran Associates, Inc., 2017.
- [28] Nikita Visnevski, Vikram Krishnamurthy, Alex Wang, and Simon Haykin. Syntactic Modeling and Signal Processing of Multifunction Radars: A Stochastic Context-Free Grammar Approach. *Proceedings of the IEEE*, 95(5):1000–1025, May 2007.
- [29] Shunjun Wei, Qizhe Qu, Hao Su, Mou Wang, Jun Shi, and Xiaojun Hao. Intra-pulse modulation radar signal recognition based on CLDN network. *IET Radar, Sonar & Navigation*, 14(6):803–810, 2020.
- [30] Shibo Yuan, Bin Wu, and Peng Li. Intra-Pulse Modulation Classification of Radar Emitter Signals Based on a 1-D Selective Kernel Convolutional Neural Network. *Remote Sensing*, 13(14):2799, January 2021.
- [31] Deguo Zeng, Hui Xiong, Jun Wang, and Bin Tang. An Approach to Intra-Pulse Modulation Recognition Based on the Ambiguity Function. *Circuits, Systems and Signal Processing*, 29(6):1103–1122, December 2010.
- [32] Jingyi Zhang, Jiaying Huang, Sheng Jin, and Shijian Lu. Vision-Language Models for Vision Tasks: A Survey. *IEEE Transactions on Pattern Analysis and Machine Intelligence*, 46(8):5625–5644, August 2024.
- [33] Yuefeng Zhao, Shengliang Han, Jimin Yang, Liren Zhang, Huaqiang Xu, and Jingjing Wang. A Novel Approach of Slope Detection Combined with Lv’s Distribution for Airborne SAR Imagery of Fast Moving Targets. *Remote Sensing*, 10(5):764, May 2018.
- [34] Mengtao Zhu, Yunjie Li, Zesi Pan, and Jian Yang. Automatic modulation recognition of compound signals using a deep multi-label classifier: A case study with radar jamming signals. *Signal Processing*, 169:107393, April 2020.
- [35] Mengtao Zhu, Ziwei Zhang, Cong Li, and Yunjie Li. JMRPE-Net: Joint modulation recognition and parameter estimation of cognitive radar signals with a deep multitask network. *IET Radar, Sonar & Navigation*, 15(11):1508–1524, 2021.
- [36] Ming Zhu, Wei-Dong Jin, Yun-Wei Pu, and Lai-Zhao Hu. Classification of radar emitter signals based on the feature of time-frequency atoms. In *2007 International Conference on Wavelet Analysis and Pattern Recognition*, volume 3, pages 1232–1236, November 2007.
- [37] Xunyu Zhu, Jian Li, Yong Liu, Can Ma, and Weiping Wang. A survey on model compression for large language models. *Transactions of the Association for Computational Linguistics*, 12:1556–1577, 2024.
- [38] Bahman Zohuri. *Radar Energy Warfare and the Challenges of Stealth Technology*. Springer, 2020.